Amino Acids (2022) 54:787–798
https://doi.org/10.1007/s00726-022-03133-9

ORIGINAL ARTICLE

First enzymological characterization of selenocysteine β-lyase from a lactic acid bacterium, *Leuconostoc mesenteroides*

Tadao Oikawa[1] · Kouhei Okajima[1] · Kazuya Yamanaka[1] · Shiro Kato[2]

Received: 15 October 2021 / Accepted: 20 January 2022 / Published online: 5 February 2022

Abstract

We succeeded in expressing selenocysteine β-lyase (SCL) from a lactic acid bacterium, *Leuconostoc mesenteroides* LK-151 (*Lm*-SCL), in the soluble fractions of *Escherichia coli* Rosetta (DE3) using a novel expression vector of pET21malb constructed by ourselves that has both maltose binding protein (MBP)- and 6 × His-tag. *Lm*-SCL acted on L-selenocysteine, L-cysteine, and L-cysteine sulfinic acid but showed a high preference for L-selenocysteine. The k_{cat} and k_{cat}/K_m values of *Lm*-SCL were determined to be 108 (min^{-1}) and 42.0 (min^{-1}•mM^{-1}), respectively, and this was enough catalytic efficiency to suggest that *Lm*-SCL might also be involved in supplying elemental selenium from L-selenocysteine to selenoproteins like other SCLs. The optimum temperature and optimum pH of *Lm*-SCL were determined to be 37 °C and pH 6.5, respectively. *Lm*-SCL was stable at 37–45 °C and pH 6.5–7.5. *Lm*-SCL was completely inhibited by the addition of hydroxylamine, semicarbazide, and iodoacetic acid. The enzyme activity of *Lm*-SCL was decreased in the presence of various metal ions, especially Cu^{2+}. The quaternary structure of *Lm*-SCL is a homodimer with a subunit molecular mass of 47.5 kDa. The similarity of the primary structure of *Lm*-SCL to other SCLs from *Citrobacter freundii*, *Escherichia coli*, humans, or mouse was calculated to be 47.0, 48.0, 12.5, or 24.0%, respectively. Unlike *Ec*-SCL, our mutational and molecular docking simulation studies revealed that C362 of *Lm*-SCL might also catalyze the deselenation of L-selenocysteine in addition to the desulfuration of L-cysteine.

Keywords Lactic acid bacteria · *Leuconostoc mesenteroides* · Selenocysteine β-lyase · Selenium metabolism

Abbreviations

DTT	Dithiothreitol
EDTA	Ethylenediamine tetraacetic acid
LB	Luria–Bertani
MRS	De Man-Rogosa-Sharpe
PCMB	*p*-Chloromercuribenzoic acid
PLP	Pyridoxal 5´-phosphate

Handling editor: S. Stuchlík.

✉ Tadao Oikawa
oikawa@kansai-u.ac.jp

[1] Department of Life Science and Biotechnology, Faculty of Chemistry, Materials and Bioengineering, Kansai University, 3-3-35 Yamate-Cho, Suita, Osaka-Fu 564-8680, Japan

[2] International Institute of Rare Sugar Research and Education, Kagawa University, 2393 Ikenobe, Miki, Kagawa 761-0795, Japan

Introduction

Selenocysteine β-lyase (SCL; EC 4.4.1.16) is classified as a Fold Type I- pyridoxal 5´-phosphate (PLP) enzyme (Eliot and Kirsch 2004) and catalyzes the conversion of L-selenocysteine into L-alanine and elemental selenium in the presence of PLP as a cofactor. SCL was first discovered in pig liver in 1982 by Professor Emeritus of Kyoto University, Dr. Kenji Soda and his colleagues (Esaki et al. 1982) and subsequently in *Citrobacter freundii* (Chocat et al. 1985), humans (Daher and Van 1992), *Escherichia coli* (Mihara et al. 1999), and *Mus musculus* (Mihara et al. 2000a, b). Mammalian SCLs are highly specific for L-selenocysteine, while bacterial SCLs, including NIFS-like proteins (Flint 1996; Zeng et al. 1993, 1994; Mihara et al. 1999), act on L-cysteine and L-selenocysteine but show a high preference for L-selenocysteine over L-cysteine. The functions of both mammalian and bacterial SCLs are considered to be involved in supplying elemental selenium produced from L-selenocysteine to the selenoproteins and elemental sulfur produced from L-cysteine for the formation of Fe-S

complexes in organisms (Lacourciere and Stadtman 1998; Kurokawa et al. 2011). A few SCLs have been crystallized, and X-ray crystallographic analysis was performed (Mihara et al. 1999; Omi et al. 2011; Collins et al. 2012; Johansson et al. 2012), but the reaction mechanism of SCL in detail is still ambiguous. SCL is a rare enzyme in nature, especially in microorganisms, and accordingly, SCL from lactic acid bacteria has not been purified and characterized thus far. During the course of our whole-genome sequence analysis of *Leuconostoc mesenteroides* LK-151, which was isolated from a Japanese sake cellar as a high producer of D-amino acids (Kato and Oikawa 2017), we found that the homologous gene of SCL existed interestingly in the genome of *L. mesenteroides* LK-151 (accession no.: AP017936).

In this manuscript, we describe the first discovery of selenocysteine *β*-lyase from a lactic acid bacterium, *Leuconostoc mesenteroides* LK-151 (*Lm*-SCL), and its enzymological properties and propose its catalytic mechanism based on mutational and docking simulation studies.

Materials and methods

Materials

Leuconostoc mesenteroides LK-151 isolated from Japanese sake cellar was kindly supplied by Kiku-Masamune Sake Brewing Co., Ltd., Hyogo, Japan. *Escherichia coli* Rosetta (DE3) and the pET21b vector were purchased from Novagen (Merck KGaA, Darmstadt, Germany). *Escherichia coli* NEB10β, pMAL-c5x vector, and T4 DNA ligase were purchased from New England BioLabs (Massachusetts, USA). L-Selenocystine (purity: > 97.0%) was purchased from Tokyo chemical Ind. Co., Ltd. (Tokyo, Japan). Protein assay CBB solution was purchased from Nacalai Tesque, Inc. (Tokyo, Japan). Ni–NTA agarose was purchased from QIAGEN (Hilden, Germany). L-Alanine dehydrogenase from *Bacillus stearothermophilus* was obtained from Nipro Corp. (Osaka, Japan). All other reagents were the best commercially available grade and purchased from Invitrogen Co. (Carlsbad, CA, USA), Kanto Chemical Co., Inc. (Tokyo, Japan), Kishida Chemical Co., Ltd. (Tokyo, Japan), Nacalai Tesque, Inc. (Kyoto, Japan), Sigma–Aldrich Co. (St. Louis, MO, USA), Tokyo chemical Ind. Co., Ltd. (Tokyo, Japan), FUJIFILM Wako Pure Chemical Corp. (Osaka, Japan), or Watanabe Chemical Ind., unless otherwise stated.

Expression of the selenocysteine *β*-lyase homologous gene from *Leuconostoc mesenteroides* LK-151

First, we constructed a new expression vector using pMAL-c5x and a pET21b vector that has both maltose binding protein (MBP)- and 6XHis-tags to express the selenocysteine β-lyase homologous gene from *Leuconostoc mesenteroides* LK-151 (*Lm-scl*) in the soluble fractions of *E. coli* Rosetta (DE3) cells under the control of the *T7-lac* promoter and purified the enzyme unless otherwise stated. From the pMAL-c5x vector, the coding region of the MBP-tag together with its ribosome binding site and factor Xa protease recognition sequence (*malE* cassette) was amplified by PCR using a set of primers as follows: MALcassette-xbaF, 5'-ATTCCCCTCTAGAATTTTCACGAGCAATTGACCAAC-3'; and MALcassette-ndeR, 5'-TGCTAGCCATATGTGAAATCCTTCCCTCGATC-3'. Underlined regions represent restriction sites for subsequent cloning. The resulting 1.2-kb fragment was digested with NdeI and XbaI and ligated with a similarly digested pET21b plasmid, yielding an MBP-tag fused protein expression vector, pET21malb, in which the *malE* cassette was placed between the *T7-lac* promoter and the multiple cloning site.

L. mesenteroides LK-151 was cultivated at 30 °C in MRS medium, and its genomic DNA was extracted using the boiling method (Sambrook et al. 1989). The *Lm-scl gene* was amplified by PCR from the genomic DNA of *L. mesenteroides* LK-151 using a pair of primers with NheI and HindIII restriction sites at the 5' and 3' termini of the gene, respectively: 5'-TTCATATGAACTATAATGCACCACA-3' and 5'-AACTCGAGTGAAACAATTATTCGT-3'. The purified PCR product and a pET21malb vector were double digested with the restriction enzymes NheI and HindIII and ligated using a T4 DNA ligase.

The DNA sequence of the pET21malb-*Lm-scl* vector constructed was confirmed, and competent *Escherichia coli* Rosetta (DE3) cells were transformed with the vector using an electroporation Gene pulser Xcell™ (Bio–Rad Laboratories, Inc., California, USA) to form pET21malb-*Lm-scl/Escherichia coli* Rosetta (DE3). The transformant obtained was cultivated in LB medium (50 mL) in a Sakaguchi flask (500 mL) containing 0.4% (*w*/*v*) glucose and 100 μg/mL carbenicillin at 37 °C until the optical density at 600 nm was reached at approximately 0.6, and *Lm*-SCL was expressed by the addition of isopropyl β-D-1-thiogalactopyranoside (0.2 mM final concentration) and further cultivation at 18 °C for 18 h.

Purification of selenocysteine *β*-lyase homolog from *Leuconostoc mesenteroides* LK-151 expressed in *Escherichia coli* Rosetta (DE3)

pET21malb-*Lm-scl/Escherichia coli* Rosetta (DE3) cells were collected by centrifugation at 7190×*g* for 15 min at 4 °C using a Centrifuge 5430R (Eppendorf, Tokyo, Japan) and suspended in 50 mM sodium phosphate buffer (NaPB), pH 8.0, containing 300 mM NaCl (buffer A) plus 10 mM imidazole (lysis buffer). This cell suspension was transferred

to a beaker PYREX® (10 mL) and treated with a sonicator (UD-201, Tomy Seiko, Tokyo) in ice-cooled water to disrupt the cells (output, 6; duty cycle, 50%). After ultrasonication, the suspension was centrifuged at 7,190×*g* for 15 min at 4 °C. The supernatant was transferred into a centrifuge tube (15 mL) (Thermo Scientific, Tokyo) to remove insoluble materials, and the supernatant was used as a cell-free extract. The cell-free extract was then applied to a column of Ni–NTA agarose (φ1.8 × 2.0 cm) (Qiagen, Hilden, Germany) that had been equilibrated with lysis buffer. The unabsorbed proteins were washed with buffer A plus 20 mM imidazole. The adsorbed protein (MBP-*Lm*-SCL) was eluted with 8 mL of buffer A plus 250 mM imidazole then collected and stored as a purified enzyme at − 80 °C after it was dialyzed against 50 mM potassium phosphate buffer (KPB), pH 7.0, containing 10% (*v*/*v*) glycerol. The purified MBP-*Lm*-SCL was treated with factor Xa to cleave the MBP-tag, if necessary. The reaction mixture (total volume: 50 µL) containing MBP-*Lm*-SCL (10 µg), Factor Xa (1 µg/µL, diluted with dilution/storage buffer (Novagen); 1 µL), Factor Xa cleavage/capture buffer (5 µL), and deionized water was incubated at 20 °C for 18 h.

Standard assay conditions

Selenocysteine β-lyase activity was assayed spectrophotometrically by measuring the amount of L-alanine produced in a reaction mixture with alanine dehydrogenase in the presence of NAD^+ according to the modified method of the manufacturer: https://www.nipro.co.jp/business/others/enzymes/nipro_enzyme_201604.pdf. The standard reaction mixture (total volume: 0.1 mL) contained 1.25 mM L-selenocysteine, 80 mM KPB (pH 6.5), 0.2 mM pyridoxal-5'-phosphate, and enzyme solution. L-Selenocysteine in the reaction mixture was prepared by reduction of L-selenocystine with DTT as follows: 12.5 mM L-selenocystine dissolved in 0.3 mL of 10 mM Tris–HCl buffer, pH 8.0, containing 0.1 M DTT was incubated at 37 °C for 60 min. The reduction of L-selenocystine to L-selenocysteine was confirmed by thin-layer chromatography (developing solvent, *n*-butyl alcohol: acetic acid: $H_2O = 4:1:1$; R_f values, L-selenocystine (0.08); L-selenocysteine (0.58)). The enzyme reaction was started by the addition of an enzyme solution containing 10 µg of purified enzyme unless otherwise stated and carried out at 37 °C for 0, 5, or 10 min. The enzyme reaction was terminated by heat treatment at 100 °C for 10 min. Then the reaction mixture (80 µL) was added to the second reaction mixture (total volume: 0.19 mL) containing 120 mM Gly-NaOH (pH 10.5) 70 µL, 10 mM NAD^+ 20 µL, and 3 U/mL L-alanine dehydrogenase 20 µL. The reaction mixture was incubated at 37 °C, and after 30 min, the absorption at 340 nm was measured using spectrophotometer UV-1800 (Shimadzu Co. Ltd, Kyoto, Japan). One unit of selenocysteine β-lyase activity is defined as the amount of enzyme that produces 1 µmol of L-alanine per min. Before carrying out the enzyme assay under various conditions, we performed preliminary experiments repeatedly to establish the optimum conditions for each enzyme assay. All calibration curves of the concentration of L-alanine (0.0–1.0 mM) versus the absorption at 340 nm used were linear with a correlation coefficient of between 0.95 and 0.99. Protein concentration was measured by the Bradford method using Protein Assay CBB solution with bovine serum albumin as a standard. All calibration curves of the concentration of protein (0–0.5 mg/mL) versus the absorption at 595 nm used were linear with a correlation coefficient of 0.99 or 1.00. The enzyme activity measured under optimal conditions and the protein concentrations were determined in two separate experiments for any given time point (this is indicated as $n = 2$) for every new batch of freshly purified MBP-*Lm*-SCL. The average value and the standard error were calculated and are shown with the equation of calibration curve and its correlation coefficient.

Basic enzymological properties

The effects of temperature and pH on MBP-*Lm*-SCL activity were examined by measuring the enzyme activity under various temperature and pH conditions. The reaction temperatures were 20, 30, 37, 40, 50, or 60 °C. The buffers used were as follows: MES (pH 5.5, 6.0, and 6.5); HEPES (pH 6.5, 7.0, 7.5, and 8.0); and TAPS (pH 8.0, 8.5, and 9.0).

The thermal and pH stabilities of MBP-*Lm*-SCL were examined by measuring the residual activity under standard assay conditions after heat or pH treatment. Heat treatment was carried out by incubating 200 µL of purified *Lm*-SCL (0.46 U/mg: mean of 0.47 and 0.45 U/mg) dissolved in 50 mM KPB (pH 7.0) at 37, 45, 50, 55, or 60 °C for 60 min. The pH treatment was carried out by mixing 100 µL of purified *Lm*-SCL (0.49 U/mg: mean of 0.48 and 0.49 U/mg) dissolved in 50 mM KPB (pH 7.0) with an equal amount of 100 mM buffer, and the mixture was incubated at 4 °C for 24 h. The buffers used were as follows: acetate (pH 5.0 and 5.5); MES (pH 5.5, 6.0 and 6.5); HEPES (pH 6.5, 7.0, 7.5 and 8.0); and TAPS (pH 8.0, 8.5 and 9.0).

The substrate specificity of MBP-*Lm*-SCL for various L-selenocysteine analogs was examined under standard assay conditions. The substrates used were L-selenocysteine, DL-selenocysteine, L-cysteine, and L-cysteine sulfinic acid.

Molecular mass and quaternary structure

The subunit molecular mass of MBP-*Lm*-SCL was determined using SDS–PAGE with a 10% T polyacrylamide gel. The purified MBP-*Lm*-SCL (20 µL) was mixed with 2 × sample buffer (20 µL) containing 125 mM Tris–HCl (pH 6.8), 4% (*w*/*v*) SDS, 10% (*w*/*v*) sucrose, 0.01% (*w*/*v*)

bromophenol blue, and 5% (*w*/*v*) (±)-dithiothreitol, and the mixture was then incubated at 95 °C for 3 min. The molecular mass of MBP-*Lm*-SCL was estimated by gel filtration. The standard proteins used were blue dextran (2000 kDa), thyroglobulin (669 kDa), ferritin (440 kDa), aldolase (158 kDa), conalbumin (75 kDa), and ovalbumin (44 kDa). Each standard protein (5.0 mg) was dissolved in 0.1 mL of Milli-Q, and the mixture was applied to a Superdex 200 column ($\varphi 10 \times 300$ mm, GE Health care, Tokyo, Japan) equilibrated with 50 mM KPB (pH 7.0). The column was eluted with the same buffer at a flow rate of 0.5 mL/min. Purified MBP-*Lm*-SCL (1.5 mg/ml, 0.1 mL) was applied to the column under the same conditions.

Kinetic analysis

Lm-SCL activity was measured with various concentrations of L-selenocysteine (0.50, 0.75, 1.00, and 1.25 mM) under standard assay conditions. The kinetic parameters (K_m and k_{cat}) of the reaction of MBP- *Lm*-SCL with L-selenocysteine were determined by analyzing the enzyme activities with Lineweaver–Burk plots (Lineweaver and Burk 1934).

Effect of inhibitors

The effects of various inhibitors on MBP-*Lm*-SCL were determined as follows: the enzyme solution (1.0 mg/mL) dissolved in 50 mM KPB (pH 7.0) + 5 mM DTT was incubated at 37 °C for 30 min with 1.0 or 10 mM of various reagents, such as L-, D-, DL-penicillamine, hydroxylamine, semicarbazide, and iodoacetic acid, and the residual activity of MBP-*Lm*-SCL was measured under standard assay conditions.

Effects of metal ions and reagents on enzyme activity

To determine the effect of metal ions and reagents on the activity of MBP-*Lm*-SCL, we measured the enzyme activity in the presence of various metal ions and reagents (final concentration: 1 mM), such as $PbCl_2$, $ZnCl_2$, $NiCl_2$, $FeCl_2$, $CuCl_2$, $MnCl_2$, $CoCl_2$, $HgCl_2$, *p*-chloromercuribenzoic acid, and ethylenediaminetetraacetic acid. MBP-*Lm*-SCL (1.12 U/mg, 180 µL) dissolved in 50 mM KPB (pH 7.0) was mixed with 20 µL of 10 mM metal ion or SH-reagent solution, and then the mixture was incubated at 4 °C for 60 min. After dialysis against 50 mM KPB (pH 7.0), the residual activity was measured under standard assay conditions.

Spectroscopic analysis

The absorption spectra of MBP-*Lm*-SCL were measured using a Hitachi U-3900H spectrophotometer at room temperature (approximately 25 °C). The holo form of MBP-*Lm*-SCL was prepared after dialysis of the purified MBP-*Lm*-SCL against 50 mM KPB, pH 7.0 (buffer B), for 16 h at 4 °C. The apo form of the enzyme was prepared after dialysis of the purified MBP-*Lm*-SCL against buffer B containing 10 mM hydroxylamine at 4 °C for 16 h. The reduced form of the enzyme was prepared after dialysis of the purified MBP-*Lm*-SCL against buffer B containing 8 mM sodium borohydride at 4 °C for 16 h.

Molecular docking of L-selenocysteine or L-cysteine to *Lm*-SCL

The Modeller program (ver. 9.23; https://salilab.org/modeller/9.23/release.html) was used for homology modeling of *Lm*-SCL with a crystal structure of *E. coli* SufS (PDB ID: 5DB5) as a template. Molecular docking of L-selenocysteine or L-cysteine to the homology model of *Lm*-SCL constructed was performed using the AutoDock Vina program (https://vina.scripps.edu). The grid box around the Schiff base of chain A was set to $24 \times 50 \times 24$ Å. The ligand molecules and side chains of H119, H120, N171, D196, Q199, S219, R357, H360, H361, C362, and R377 of chain A and H51, E250, and T273 of chain B were allowed to be flexible during the simulation.

Analysis of protein sequence alignment

Analysis of protein sequence alignment was carried out using Jalview (https://www.jalview.org) (Waterhouse et al. 2009). The secondary structure was predicted via a jury network (Cuff and Barton 1999; Cole et al. 2008).

Site-directed mutagenesis

The amino acid residues H119, E250, C362, and R377, which are candidate catalytic residues of *Lm*-SCL predicted from the protein sequence alignment and the molecular docking studies, were replaced singly or doubly with an alanine residue to produce H119A, C362A, R377A, H119A/C362A, and E250A/C362A-*Lm*-SCL by site-directed mutagenesis according to the method of Takara Bio Inc. (Kyoto, Japan). The primers used are summarized in Table 1. PCR was carried out in a reaction mixture (total volume: 20 µL) containing Prime STAR MAX Premix (10 µL), 10 µM forward primer (0.4 µL), 10 µM reverse primer (0.4 µL), pET21malb-*lm-scl* (< 0.1 µL), and Milli-Q (9.2 µL). The PCR mixture was transformed into *Escherichia coli* NEB10β, and each transformant harboring the desired mutated plasmid was cultivated and purified according to the method mentioned above. The activities of each mutated enzyme were measured under standard assay conditions.

Table 1 Primer sequences used for construction of mutated *Lm*-SCLs

Constructed plasmid	Mutation point	Primer sequence
pETMALb-*lm-scl*-H119A pETMALb-*lm-scl*-H119A/C362A	H119	Forward: 5'-atggaagcccattctaatattgtgccg-3' Reverse: 5'-agaatgggcttccatgtaagatattag-3'
pETMALb-*lm-scl*-C362A pETMALb-*lm-scl*-H119A/C362A pETMALb-*lm-scl*-E250A/C362A	C362	Forward: 5'-catcatgccgcgcagccgctgatgaaa-3' Reverse: 5'-ctgcgcggcatgatgtcctgcacgaac-3'
pETMALb-*lm-scl*-R377A	R377	Forward: 5'-acagttgccattagtttgtatatctat-3' Reverse: 5'-actaatggcaactgtcgctgcaatatt-3'
pETMALb-*lm-scl*-E250A/C362A	E250	Forward: 5'-ggtggagcgatgattgaattggtagac-3' Reverse: 5'-aatcatcgctccaccaaattgagcagg-3'

Underline in the Table means mutation point

Phylogenetic tree analysis

Phylogenetic analysis was carried out using the primary structures of *Lm*-SCL and 23 representative proteins homologous to *Lm*-SCL. The phylogenetic tree was made by the neighbor-joining method (Saitou and Nei 1987) using Protein BLAST Tree View based on the results of BLAST pairwise alignments. The analytical conditions used were as follows: max sequence difference, 0.85; and distance, Grishin (protein).

Accession number

The DNA sequence of the gene encoding the selenocysteine β-lyase and the genome from *Leuconostoc mesenteroides* LK-151 are available at GenBank under accession no. LC652838 and AP017396, respectively.

Results

Expression and purification of MBP-*Lm*-SCL

First, we tried to express *Lm-scl* using pET21b, but almost all of its gene product, *Lm*-SCL, is expressed in the insoluble fraction of *E. coli* BL21 (DE3) cells. Therefore, we constructed the new MBP-tag fused protein expression vector pET21malb, and using pET21malb, we succeeded in expressing MPB-*Lm*-SCL in a soluble fraction of *E. coli* BL21 (DE3) cells and purified it homogeneously (Supplemental Fig. 1). The results of purification of MBP-*Lm*-SCL are summarized in Table 2.

Effect of MBP-tag on the enzyme activity of *Lm*-SCL

We measured the enzyme activities with MPB-*Lm*-SCL or Factor Xa-treated MPB-*Lm*-SCL, that is, *Lm*-SCL, to confirm the effect of the MBP tag on the enzyme activity of *Lm*-SCL. The selenocysteine β-lyase activity of MPB-*Lm*-SCL (0.47 U/mg: mean of 0.45 and 0.48 U/mg) is almost same as that of *Lm*-SCL (0.49 U/mg: mean of 0.48 and 0.49 U/mg), and accordingly, we decided to use MPB-*Lm*-SCL to measure various enzymological properties of *Lm*-SCL except its quaternary structure. Hereafter we use the word *Lm*-SCL instead of MPB-*Lm*-SCL to describe the experiment with MPB-*Lm*-SCL in this manuscript.

Substrate specificity of *Lm*-SCL

Table 3 shows the substrate specificity of *Lm*-SCL. *Lm*-SCL acts on L-selenocysteine, L-cysteine, and L-cysteine sulfinic acid but shows a high preference for L-selenocysteine.

Table 2 Purification of *Lm*-SCL

Step	Total activity (U)			Total protein (mg)			Specific activity (U/mg)			Yield (%)	Fold (–)
	1	2	Mean	1	2	Mean	1	2	Mean		
Cell-free extract	4.28	6.21	5.25	61.2	59.4	60.3	0.07	0.10	0.09	100	1
Ni–NTA column chromatography	0.36	0.41	0.39	1.4	1.7	1.5	0.24	0.27	0.26	7	3

The calibration curve of the concentration of L-alanine (0.0–1.0 mM) versus the absorption at 340 nm used is $y = 1.15x$ ($R^2 = 0.97$). The calibration curve of the concentration of protein (0–0.5 mg/mL) versus the absorption at 595 nm used is $y = 1.09x$ ($R^2 = 1.00$). Data obtained from two separate experiments under optimum conditions established based on preliminary experiments and its mean are shown

Table 3 Substrate specificity of *Lm*-SCL

Substrate	Specific activity (U/mg)			Relative activity (%)
	1	2	Mean	
L-Selenocysteine	0.37	0.35	0.36	100
DL-Selenocysteine	0.32	0.38	0.35	97
L-Cysteine	0.05	0.06	0.06	17
L-Cysteine sulfinic acid	0.04	0.04	0.04	11

The calibration curve of the concentration of L-alanine (0.0–1.0 mM) versus the absorption at 340 nm used is $y = 1.15x$ ($R^2 = 0.97$). The calibration curve of the concentration of protein (0–0.5 mg/mL) versus the absorption at 595 nm used is $y = 1.09x$ ($R^2 = 1.00$). Data obtained from two separate experiments under optimum conditions established based on preliminary experiments and its mean are shown

Basic enzymatic properties

The optimum temperature and pH of *Lm*-SCL were determined to be 37 °C and pH 6.5, respectively (Supplemental Fig. 2). *Lm*-SCL is stable between 37 and 45 °C and pH 6.5–7.5 and shows more than 60% and 50% activity, respectively, compared with the enzyme without heat or pH treatment (Supplemental Fig. 3). The treatment with hydroxylamine, semicarbazide, and iodoacetic acid completely inhibit *Lm*-SCL. *Lm*-SCL is strongly inhibited in the presence of L-, D-, and DL-penicillamine (Supplemental Table 1). The enzyme activity of *Lm*-SCL is decreased in the presence of various metal ions, especially Cu^{2+}, Ca^{2+}, Al^{3+}, Mn^{2+}, and Hg^{2+} (Supplemental Table 2). The kinetic parameters of *Lm*-SCL were determined and are summarized with those of other SCLs in Table 4. The quaternary structure of *Lm*-SCL is a homodimer with a subunit molecular mass of 47.5 kDa.

Primary structure of *Lm*-SCL

The primary structure of *Lm*-SCL was compared with that of other mammalian and bacterial SCLs previously reported (Fig. 1). The similarities between *Lm*-SCL and SCL from *Citrobacter freundii* (accession number: WP_038640267, *Cf*-SCL), *Escherichia coli* (accession number: 1JF9_A, *Ec*-SCL), humans (accession number: NP_057594, Human-SCL), or mouse (accession number: NP_057926, Mouse-SCL) were calculated to be 47.0, 48.0, 12.5, or 24.0%, respectively. The PLP-binding lysine residue of *Lm*-SCL is considered to be K222, and it is conserved between mammalian and bacterial SCLs (Fig. 1). The catalytic residues of *Ec*-SCL, i.e., H123, C364, and R379 are well conserved in the primary structure of *Lm*-SCL as H119, C362, and R377, respectively.

Molecular docking of substrates to *Lm*-SCL

We performed molecular docking simulations to estimate the substrate binding of L-selenocysteine and L-cysteine molecules to the active center of *Lm*-SCL using the program AutoDock Vina (Fig. 2). All amino acid residues conserved in the primary structure of *Lm*-SCL, i.e., H119, K222, C362, and R377 exist in the active center of *Lm*-SCL when either L-selenocysteine or L-cysteine docked as a substrate. Accordingly, K222 is predicted strongly as the PLP-binding lysine residue of *Lm*-SCL by the molecular docking simulations. Interestingly, we found that E250 of *Lm*-SCL exists near a substrate molecule that is conserved with mammalian SCLs (human and mouse SCLs) but is replaced with a serine residue in the primary structure of bacterial SCLs (*Cf*- and *Ec*-SCLs) (Fig. 1). The side chain of E250 of *Lm*-SCL moves only when an L-cysteine molecule docks as a substrate (Fig. 2).

Table 4 Kinetic parameters of *Lm*-SCL

	V_{max} (U/mg)			k_{cat} (min^{-1})			K_m (mM)			k_{cat}/K_m (min^{-1}•mM^{-1})		
	1	2	Mean	1	2	Mean	1	2	Mean	1	2	Mean
Lm-SCL	2.83	2.32	2.58	109	106	108	2.66	2.49	2.58	41.1	42.8	42.0
Ec-SCL	6.8			–			2.6			–		
Cf-SCL	9.49			–			0.95			–		
Human-SCL	-			–			0.5			–		
Mouse-SCL	58			2,760			9.9			278.8		

The calibration curve of the concentration of L-alanine (0.0–1.0 mM) versus the absorption at 340 nm used $y = 0.684x$ ($R^2 = 0.99$). The calibration curve of the concentration of protein (0–0.5 mg/mL) versus the absorption at 595 nm used is $y = 1.09x$ ($R^2 = 1.00$). Data obtained from two separate experiments under optimum conditions established based on preliminary experiments and its mean are shown. The data of *Ec*-SCL, *Cf*-SCL, Human-SCL, and Mouse-SCL are reproduced from references, Mihara et al. (2000a, b), Chocat et al. (1985), and Daher and Lente (1992), respectively

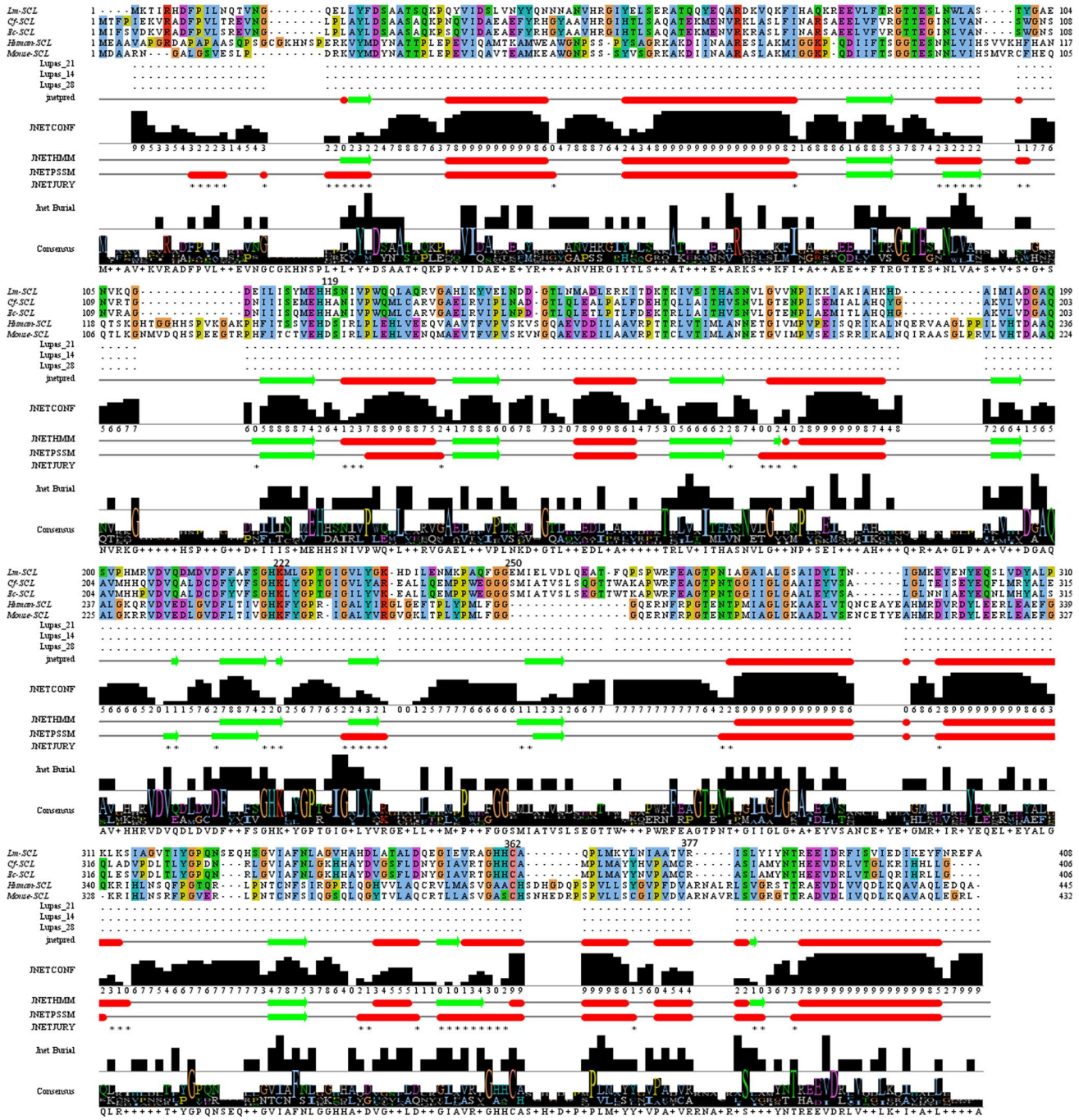

Fig. 1 Alignment of the primary structure of *Lm*-SCL. The colors in the primary structures indicate the character of sidechain of amino acid residues and specific amino acids as follows: ■: hydrophobic, ■ : cationic, ■: anionic, ■: polar, ■: G, ■: P, ■: H and Y. Jnetpred: the consensus prediction. Helices are marked as red tubes, and sheets are marked as light green arrows. JNETCONF: the confidence estimates for the prediction. High values mean high confidence. JNETHMM: the HMM profile-based prediction. Helices are marked as red tubes, and sheets are marked as light green arrows. JNETPSSM: the PSSM profile-based prediction. Helices are marked as red tubes, and sheets are marked as light green arrows. JNETJURY: An asterisk in this annotation indicates that JNETJURY was invoked to rationalize significantly different primary predictions. Jnet Burial: prediction of solvent accessibility

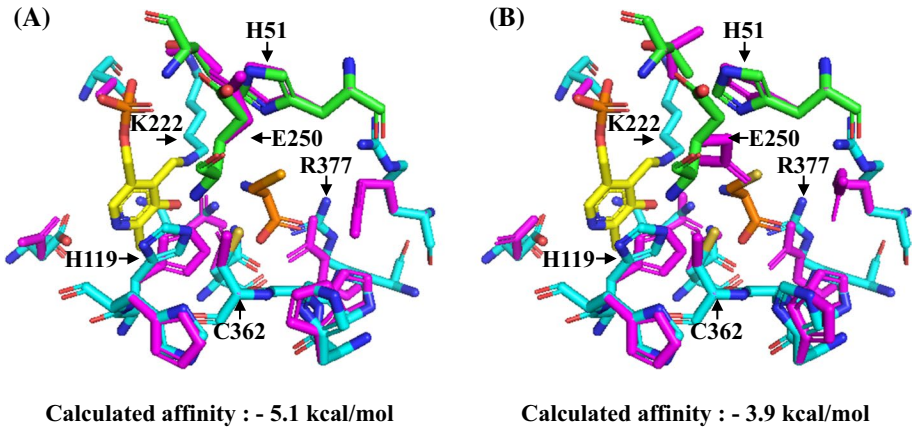

Fig. 2 Molecular models of the substrate in the active center of *Lm*-SCL. The binding modes for *Lm*-SCL and L-selenocysteine (**A**) and L-cysteine (**B**) calculated by AutoDock Vina were visualized using PyMOL software. Carbon atoms of chains A and B of *Lm*-SCL, PLP molecules bound to K222 of chain A, and ligand molecules are shown in blue, green, yellow, and orange, respectively. Flexible residues during the simulation are shown in magenta. The binding affinities calculated from this simulation are noted below each image

Table 5 Comparison of specific activities of *Lm*-SCL and its mutated enzymes

	Specific activity(U/mg)			Relative activity (%)
	1	2	Mean	
Lm-SCL	0.95	1.21	1.08	100
Lm-SCL-H119A	0.05	0.08	0.07	7
Lm-SCL-C362A	0.77	0.75	0.76	70
Lm-SCL-R377A	0.00	0.00	0.00	0
Lm-SCL-H119A/C362A	0.00	0.00	0.00	0
Lm-SCL-E250A/C362A	0.70	0.76	0.73	68

The calibration curve of the concentration of L-alanine (0.0–1.0 mM) versus the absorption at 340 nm used for *Lm*-SCL, *Lm*-SCL-H119A, *Lm*-SCL-C362A, *Lm*-SCL-R377A, & *Lm*-SCL-H119A/C362A and *Lm*-SCL-E250A/C362A are $y=1.15$x ($R^2=0.97$) and $y=0.95x$ ($R^2=0.99$), respectively. The calibration curve of the concentration of protein (0–0.5 mg/mL) versus the absorption at 595 nm used for *Lm*-SCL, *Lm*-SCL-H119A, *Lm*-SCL-C362A, *Lm*-SCL-R377A, & *Lm*-SCL-H119A/C362A and *Lm*-SCL-E250A/C362A are $y=1.09x$ ($R^2=1.00$) and $y=x$ ($R^2=1.00$), respectively. Data obtained from two separate experiments under optimum conditions established based on preliminary experiments and its mean are shown

Comparison of enzymatic activities and spectral features between *Lm*-SCL and various mutated *Lm*-SCLs

The SCL activities were compared using *Lm*-SCL and its mutated enzymes (Table 5). The SCL activity of *Lm*-SCL-H119A decreases dramatically (specific activity 0.07 U/mg), and this observation agrees well with *Ec*-SCL-H123A. The SCL activity of *Lm*-SCL-C362A decreased slightly (specific activity 0.76 U/mg), while *Ec*-SCL-C364A shows approximately 1.5 times higher SCL activity than *Ec*-SCL. We found that *Lm*-H119A/C362A shows no enzyme activity toward L-selenocysteine, but *Lm*-SCL-E250A/C362A shows almost the same activity as *Lm*-SCL-C362A. *Lm*-SCL-R377A also have no SCL activity similar to *Ec*-SCL-R379A.

The absorption spectra of the holo-, apo-, and reduced forms of *Lm*-SCL were measured (Fig. 3A). The absorption maximum at 420 nm, which is derived from an internal aldimine linkage probably between K222 and PLP, is observed for *Lm*-SCL, and the ratio of A_{280} to A_{420} is approximately 12.8. This observation suggests that *Lm*-SCL binds PLP as a coenzyme. Compared with the absorption spectrum of the holo-form of *Lm*-SCL with that of *Lm*-SCL-H119A, C362A, and R377A, the absorption maximum at 420 nm decreases significantly in *Lm*-SCL-H119A and slightly in *Lm*-SCL-C362A. However, unexpectedly, in the case of *Lm*-SCL-R377A, the absorption maximum at 420 nm is similar to that of *Lm*-SCL (Fig. 3B).

Phylogenetic analysis of *Lm*-SCL

The Protein BLAST search shows that the homologous protein whose identity is over 62% similar to the primary structure of *Lm*-SCL exists in very restricted lactic acid bacteria. The phylogenetic tree of *Lm*-SCL based on the results of the Protein BLAST shows that the homologs of *Lm*-SCL form only the cluster with the proteins derived from various species of *Leuconostoc*, such as *L. palmae*, *L. holzapfelii, L. carnosum, L. gelidum, L. inhae, L. miyukkimuchii, L. suionicum, L. litchi, L. pseudomesenteroides, L. falkenbergense, L. rapi,* and *L. fallax* (Fig. 4).

Discussion

L-Selenocysteine β-lyase is a rare enzyme in nature, especially in bacteria. Two bacterial SCLs, namely those from *Citrobacter freundii* and *Escherichia coli* have been purified

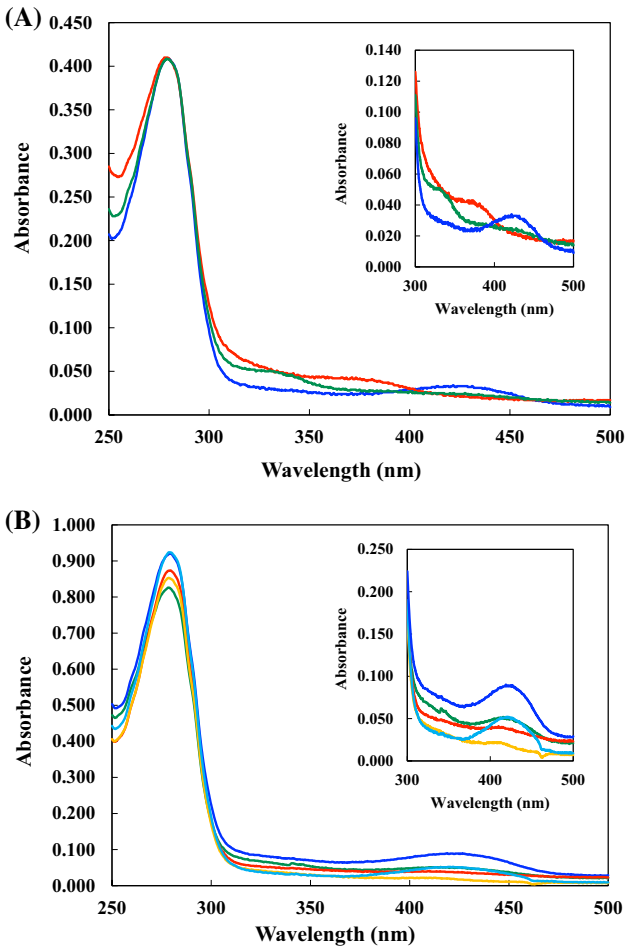

Fig. 3 Spectroscopic analysis of *Lm*-SCL and its mutated enzymes. **A** Absorption spectra of holo, apo, and reduced forms of *Lm*-SCL. Blue line, holo form; Green line, apo form; Red line, reduced form. The protein concentration was as follows: holo form, 0.44 mg/mL; apo form, 0.36 mg/mL; reduced form 0.37 mg/mL. The buffer used was 50 mM KPB (pH 7.0). **B** Comparison of the absorption spectrum of the holo-form of *Lm*-SCLwith that of *Lm*-SCL-H119A, C362A, R377A, and H119A/C362A. Blue line, *Lm*-SCL; Green line, *Lm*-SCL-C362A; Red line, *Lm*-SCL-H119A; Pale blue, *Lm*-SCL-R377A, Yellow, *Lm*-SCL-H119A/C362A. The protein concentration was as follows: *Lm*-SCL, 0.59 mg/mL; *Lm*-SCL-C362A, 0.54 mg/mL; *Lm*-SCL-H119A, 0.49 mg/mL; *Lm*-SCL-R377A, 0.51 mg/mL; *Lm*-SCL-H119A/C362A, 0.51 mg/mL. The buffer used was 50 mM KPB (pH 7.0)

and characterized enzymologically (Chocat et al. 1985; Mihara et al. 1999). We succeeded in expressing selenocysteine β-lyase (SCL) from a lactic acid bacterium, *Leuconostoc mesenteroides* LK-151 (*Lm*-SCL), in the soluble fractions of *Escherichia coli* Rosetta (DE3) using a novel expression vector of pET21malb constructed by ourselves that has both maltose binding protein (MBP)- and 6×His-tag. To our knowledge, this is the first example of SCL from a lactic acid bacterium and is also a rare example in entire organisms.

Lm-SCL acts on L-selenocysteine, L-cysteine, and L-cysteine sulfinic acid but showed a high preference for L-selenocysteine, similar to other bacterial SCLs (Table 3), and the value of the *Vmax* of *Lm*-SCL (2.58 U/mg) is similar to other bacterial SCLs, such as *Ec*-SCL (6.8 U/mg) and *Cf*-SCL (9.49 U/mg) (Table 4). The k_{cat}/K_m of *Lm*-SCL (42.8 min^{-1}•mM^{-1}) is comparable that of mouse-SCL (278.8 min^{-1}•mM^{-1}) (Table 4). This was enough activity to suggest that *Lm*-SCL might also be involved in supplying elemental selenium from L-selenocysteine to selenoproteins and elemental sulfur produced from L-cysteine for the formation of Fe-S complexes in organisms such as other SCLs (Lacourciere and Stadtman 1998; Kurokawa et al. 2011).

In the genome of *L. mesenteroides* LK-151 near *Lm-scl* (locus_tag: LEMES_00197), the genes encoding putative Fe-S cluster formation protein, NifU-like (LEMES_00196) and putative metal-sulfur cluster biosynthetic protein (LEMES_00194) existed, and whose gene products are expected to be involved in a selenium and sulfur metabolism of *L. mesenteroides* LK-151 and supports this hypothesis (Pilon-Smits et al. 2002).

Mihara et al. reported that C364 of *Ec*-SCL was not essential for the catalytic activity toward L-selenocysteine but is for L-cysteine (Mihara et al. 2002). They proposed that the reaction mechanism of *Ec*-SCL with L-selenocysteine is different from that with L-cysteine, and the difference is attributed to the difference in pK values between the selenohydryl group of L-selenocysteine and the thiol group of L-cysteine. The deselenation of L-selenocysteine occurs spontaneously from the ketimine intermediate of PLP and L-selenocysteine because the pK value of the selenohydryl group of L-selenocysteine (pK = 5.2) is much lower than the pH of the reaction mixture they used (pH = 7.4). However, the pK value of the thiol group of L-cysteine (pK = 8.3) is higher than pH 7.4, and the desulfuration of L-cysteine requires nucleophilic attack by C364 of *Ec*-SCL. However, our mutational study revealed that C362 of *Lm*-SCL corresponding to C364 of *Ec*-SCL may also catalyze the deselenation of L-selenocysteine in addition to the desulfuration of L-cysteine. The observed difference is probably attributed to the difference in pH of the assay mixture: pH 7.4 for *Ec*-SCL and pH 6.5 for *Lm*-SCL. The optimum pH of *Lm*-SCL (pH = 6.5) is lower than that of *Ec*-SCL (pH = 7.5) and is near the pK value of the selenohydryl group of L-selenocysteine. This characteristic pH profile of *Lm*-SCL may reveal a new aspect of the function of C362 in a bacterial SCL. Accordingly, we propose that the deselenation of L-selenocysteine catalyzed by *Lm*-SCL proceeds through two reaction mechanisms both with (Fig. 5A) and without (Fig. 5B) nucleophilic attack by C362 of *Lm*-SCL.

Our docking simulation study showed that the positions of amino acid residues surrounding L-selenocysteine and L-cysteine molecules in the active center of *Lm*-SCL are not

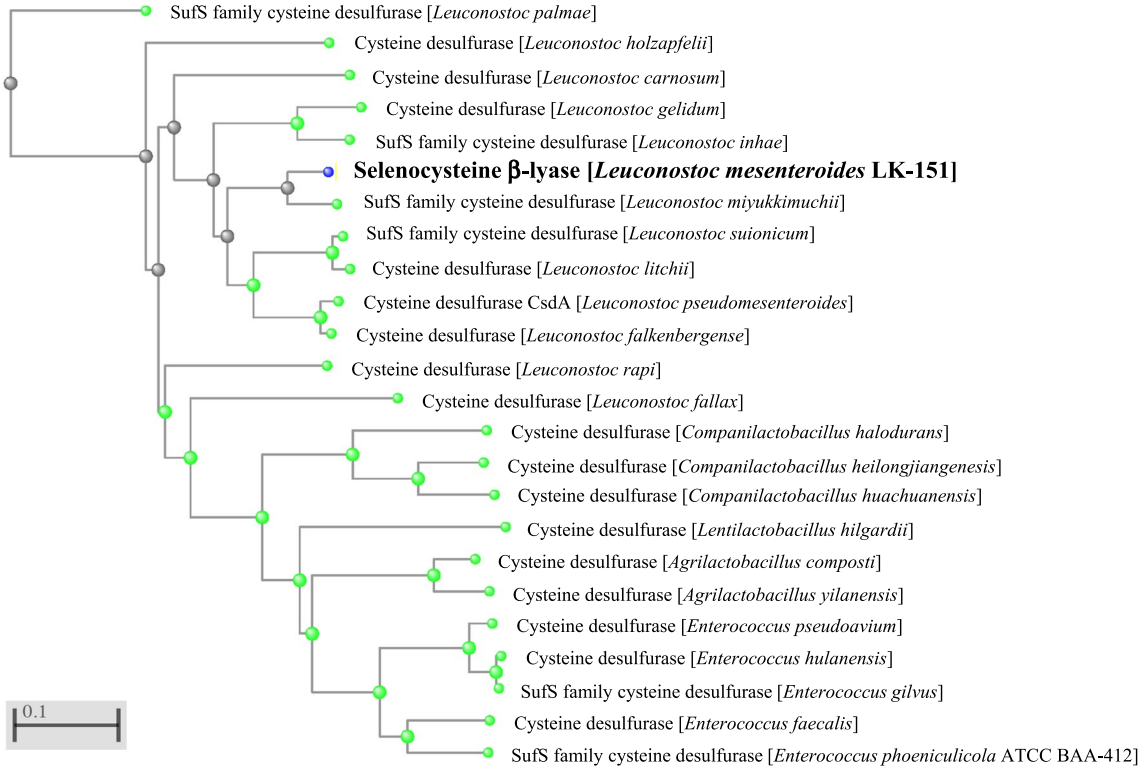

Fig. 4 Phylogenetic analysis of *Lm*-SCL. The phylogenetic analysis was carried out using the following sequences (accession no; identity for *Lm*-SCL): *Leuconostoc miyukkimuchii* (WP_220740652.1; 91.7%), *Leuconostoc suionicum* (WP_211636978.1; 82.8%), *Leuconostoc litchii* (WP_148606558.1; 82.4%), *Leuconostoc pseudomesenteroides* (TOZ08121.1; 80.6%), *Leuconostoc falkenbergense* (WP_188356479.1; 80.6%), *Leuconostoc gelidum* (WP_060391196.1; 77.5%), *Leuconostoc inhae*. (WP_220734553.1; 77.6%), *Leuconostoc rapi* (WP_204769388.1; 72.5%), *Leuconostoc carnosum* (WP_150280309.1; 74.0%), *Leuconostoc holzapfelii* (WP_168676043.1; 70.2%), *Leuconostoc palmae* (WP_220741874.1; 65.9%), *Agrilactobacillus composti* (WP_057002295.1; 63.8%), *Companilactobacillus halodurans* (WP_153522285.1; 64.3%), *Enterococcus hulanensis* (WP_206916504.1; 63.8%), *Enterococcus faecalis* (EGO6530340.1; 63.3%), *Enterococcus gilvus* (WP_221676086.1; 63.8%), *Companilactobacillus heilongjiangensis* (WP_041499075.1; 65.0%), *Enterococcus phoeniculicola* ATCC BAA-412 (EOL41599.1; 62.8%), *Agrilactobacillus yilanensis* (WP_125713532.1; 62.5%), *Companilactobacillus huachuanensis* (WP_137611559.1; 63.5%), *Lentilactobacillus hilgardii* (WP_003557453.1; 63.4%), and *Enterococcus pseudoavium* (WP_115872699.1; 64.8%)

very different from each other (Fig. 2). Only the side chain position of E250 is estimated to be different, but our mutational study of E250 of *Lm*-SCL showed that E250 is not involved in the SCL activity of *Lm*-SCL. Recently, H55 in the active center of *Ec*-SCL studied as SufS of *Escherichia coli* has been confirmed to be dispensable for the catalytic activity of the desulfuration of L-cysteine by preparation of H55A mutated enzyme (Dunkle et al. 2019). H55 of *Ec*-SCL is also shown to be not essential for the catalytic activity of the deselenation of L-selenocysteine previously (Mihara et al. 2002). H55 of *Ec*-SCL forms a hydrogen bond to S254 in the active center, but the disruption of this hydrogen bond does not cause a broader structural change. Interestingly, H55 and S254 of *Ec*-SCL are conserved as H51 and E250 of *Lm*-SCL, respectively. Considering the structural similarity in the active center between *Lm*-SCL and *Ec*-SCL, the hydrogen bond is probably made between H51 and E250 of *Lm*-SCL, and in addition to E250 based on our mutational study, H51 is considered to be uninvolved in the SCL activity of *Lm*-SCL.

Several lactic acid bacteria have been reported to take up the inorganic selenium of selenous acid and convert it to elemental selenium or organic selenium (L-selenocysteine or L-selenomethionine) to accumulate Se in their cells (Kurek et al. 2016; Kousha et al. 2017; Etgeton et al. 2018). However, the selenium metabolism of lactic acid bacteria has not been clarified at all at the enzyme molecular level. Our phylogenetic analysis showed that the homologous proteins of *Lm*-SCL distribute in very restricted lactic acid bacteria, especially various species of *Leuconostoc*, and these lactic acid bacteria may metabolize inorganic and/or organic selenium. Our new finding of SCL in lactic acid bacteria aids in the elucidation of future unknown selenium metabolism of lactic acid bacteria.

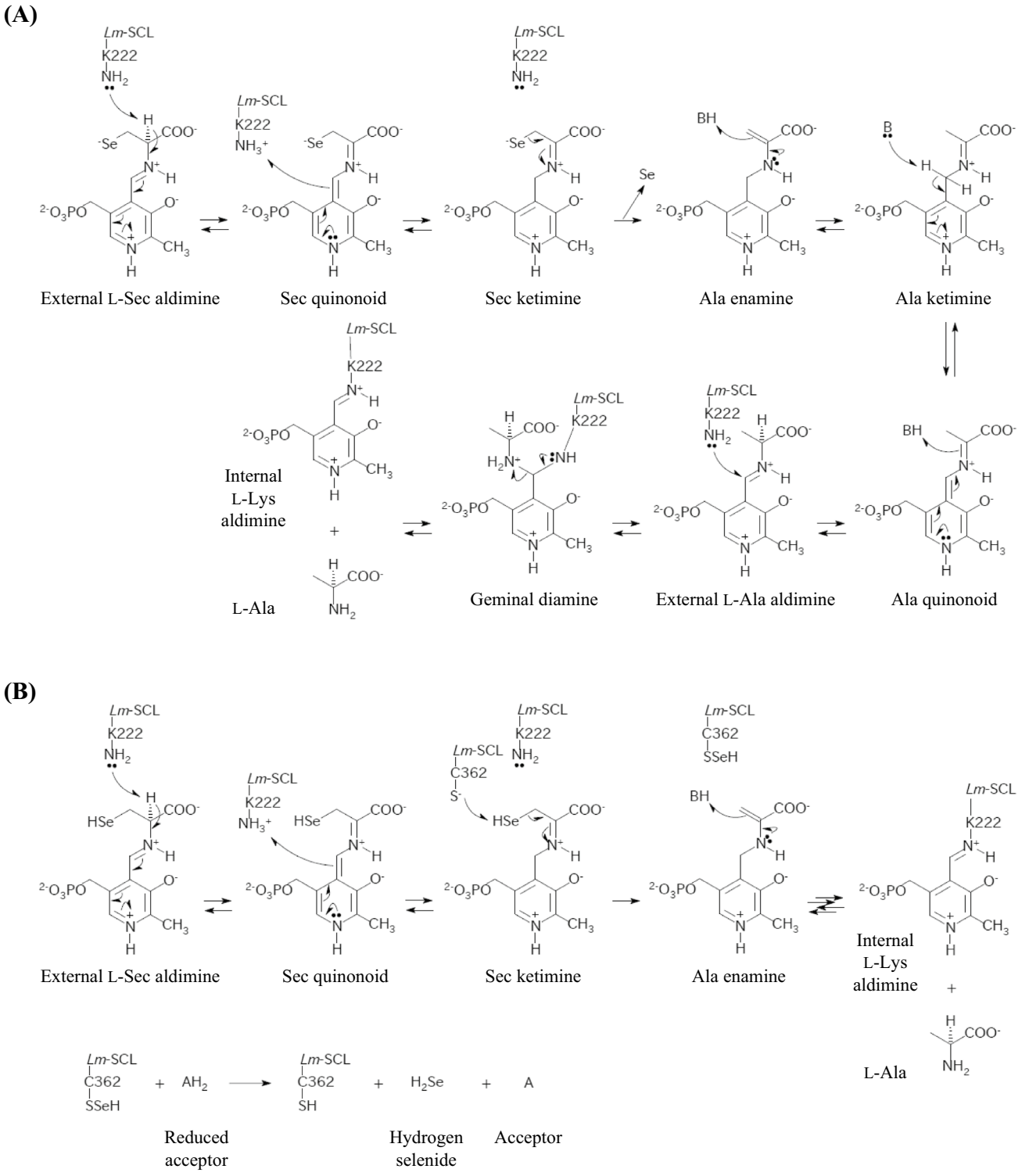

Fig. 5 Proposed reaction mechanism of *Lm*-SCL. **A** Without nucleophilic attack by Cys362. **B** With nucleophilic attack by Cys362

Supplementary Information The online version contains supplementary material available at https://doi.org/10.1007/s00726-022-03133-9.

Acknowledgements We thank Mr. Takumi Matsumura for the construction of pET21malb-*Lm-scl* and detection of the SCL activity of *Lm*-SCL. We appreciate the contribution of Ms Chihiro Kasahara for the preparation of E250A/C362A-*Lm*-SCL and evaluation of its SCL activity. We thank Dr. Takashi Kimura (Nipro Corp., Osaka, Japan) for his kind gift of L-alanine dehydrogenase of *Bacillus stearothermophilus*.

Author contributions TO designed and supervised the studies. TO, KO, KY, and SK wrote first manuscript. KO and KY carried out the experiments. TO and SK performed the primary structure and phylogenetic analyses. SK carried out the molecular docking simulation. TO and SK deduced the reaction mechanism. TO wrote the revised manuscripts.

Declarations

Conflict of interest The authors declare that they have no conflicts of interest.

Ethical approval This manuscript does not contain any studies with human participants or animals performed by any of the authors.

References

Andrew EC, Jack KF (2004) Pyridoxal phosphate enzymes: mechanistic, structural, and evolutionary considerations. Annu Rev Biochem 73:383–415

Chocat P, Esaki N, Tanizawa K, Nakamura K, Tanaka H, Soda K (1985) Purification and characterization of selenocysteine β-lyase from *Citrobacter freundii*. J Bacteriol 163:669–676

Cole C, Barber JD, Barton GJ (2008) The Jpred 3 secondary structure prediction server. Nucleic Acids Res 36:W197–W201

Collins R, Johansson A-L, Karlberg T, Markova N, van den Berg S, Olesen K, Hammarström M, Flores A, Schüler H, Schiavone HL, Brzezinski P, Arnér ESJ, Högbom M (2012) Biochemical discrimination between selenium and sulfur 1: a single residue provides selenium specificity to human selenocysteine lyase. ProS One 7:e30581

Cuff JA, Barton GJ (1999) Application of enhanced multiple sequence alignment profiles to improve protein secondary structure prediction. Proteins 40:502–511

Daher R, Lente FV (1992) Characterization of selenocysteine lyase in human tissues and its relationship to tissue selenium concentrations. J Trace Elem Electrolytes Health Dis 6:1890194

Daher R, Van LF (1992) Characterization of selenocysteine lyase in human tissues and its relationship to tissue selenium concentrations. J Trace Elem Electrolytes Health Dis 6:189–194

Dunkle JK, Bruno M, Outten W, Frantom PA (2019) Structural evidence for dimer-interface driven regulation of the type II cysteine desulfurase, SufS. Biochemistry 58:687–696

Esaki N, Nakamura T, Tanaka H, Soda K (1982) Selenocysteine lyase, a novel enzyme that specifically acts on selenocysteine. mammalian distribution and purification and properties of pig liver enzyme. J Biol Chem 257:4386–4391

Etgeton HP, Altmayer T, Gonçalves TE, Schweizer YA, Oreste EQ, Ribeiro AS, Lehn DN, Volken de Souza CF, Hoehne L (2018) Assessment of selenium bioaccumulation in lactic acid bacteria. J Dairy Sci 101:10626–10635

Flint DH (1996) *Escherichia coli* contains a protein that is homologous in function and N-terminal sequence to the protein encoded by the NIFS gene of *Azotobacter vinelandii* and that can participate in the synthesis of the FeS cluster of dihydroxy acid dehydratase. J Biol Chem 271:16068–16074

Johansson A-L, Karlberg T, Collins R, Arnér ESJ, Brzezinski P, Högbom M (2012) Biochemical discrimination between selenium and sulfur 2: mechanistic investigation of the selenium specificity of human selenocysteine lyase. ProS One 7:e30528

Kato S, Oikawa T (2017) Genome sequence of *Leuconostoc mesenteroides* LK-151 isolated from a Japanese sake cellar as a high producer of D-amino acids. Genome Announc 30:e00661 (**e717**)

Kousha M, Yeganeh S, Keramat Amirkolaie A (2017) Effect of sodium selenite on the bacteria growth, selenium accumulation, and selenium biotransformation in *Pediococcus acidilactici*. Food Sci Biotechnol 26:1013–1018

Kurek E, Ruszczyńska A, Wojciechowski M, Łuciuk A, Michalska-Kacymirow M, Motyl I, Bulska E (2016) Bio-transformation of seleniuim in Se-enriched bacterial strains of *Lactobacillus casei*. Rocz Panstw Zakl Hig 67:253–262

Kurokawa S, Takehashi M, Tanaka H, Mihara H, Kurihara T, Tanaka S, Hill K, Burk R, Esaki N (2011) Mammalian selenocysteine lyase is involved in selenoprotein biosynthesis. J Nutr Sci Vitaminol 57:298–305

Lacourciere Gerard M, Stadtman Thressa C (1998) The NIFS protein can function as a selenide delivery protein in the biosynthesis of selenophosphate. J Biol Chem 273:30921–30926

Lineweaver H, Burk D (1934) The determination of enzyme dissociation constants. J Am Chem Soc 56:658–666

Mihara H, Maeda M, Fujii T, Kurihara T, Hata Y, Esaki N (1999) A *nifS*-like gene, *csdB*, encodes an *Escherichia coli* counterpart of mammalian selenocysteine lyase. J Biol Chem 274:14768–14772

Mihara H, Kurihara T, Watanabe T, Yoshimura T, Esaki N (2000a) cDNA cloning, purification, and characterization of mouse liver selenocysteine lyase. candidate for selenium delivery protein in selenoprotein symthesis. J Biol Chem 275:6195–6200

Mihara H, Kurihara T, Yoshimura T, Esaki N (2000b) Kinetic and mutational studies of three NifS homologs from *Escherichia coli*: mechanistic difference between L-cysteine desulfurase and L-selenocysteine lyase reactions. J Biochem 127:559–567

Mihara H, Fujii T, Kato S, Kurihara T, Hata Y, Esaki N (2002) Structure of externl aldimine of *Escherichia coli* CsdB, an IscS/NifS homolog: implications for its specificity toward selenocysteine. J BioChem 131:679–685

Omi S, Kurokawa S, Mihara H, Hayashi H, Goto M, Miyahara I, Kurihara T, Hirotsu K, Esaki N (2011) Reaction mechanism and molecular basis for selenium/sulfur discrimination of selenocysteine lyase. J Biol Chem 285:12133–12139

Pilon-Smits EAH, Garifullina GF, Abdel-Ghany S, Kato S, Mihara H, Hale KL, Burkhead JL, Esaki N, Kurihara T, Pilon M (2011) Characterization of a NifS-like chloroplast protein from Arabidopsis. Implications for its role in sulfur and selenium metabolism. Plant Physiol 130:1309–1318

Saitou N, Nei M (1987) The neighbor-joining method: a new method for reconstructing phylogenetic trees. Mol Biol Evol 4:406–425

Sambrook J, Fritsch EF, Maniatis T (1989) Molecular cloning. Cold spring harbor laboratory press, New York

Waterhouse AM, Procter JB, Martin DMA, Clamp M, Barton GJ (2009) Jalview version 2—a multiple sequence alignment editor and analysis workbench. Bioinformatics 25:1189–1191

Zeng L, White RH, Cash VL, Jack RF, Dean DR (1993) Cysteine desulfurase activity indicates a role for NIFS in metallocluster biosynthesis. Proc Natl Acad Sci USA 90:2754–2758

Zeng L, White RH, Cash VL, Dean DR (1994) Mechanism for the desulfurization of L-cysteine catalyzed by the NIFS gene product. Biochemistry 33:4714–4720